This article has been accepted for inclusion in a future issue of this journal. Content is final as presented, with the exception of pagination.

Mechanism for Unipolar Reset in Negative Thermophoresis Resistive Memory Devices

Xu Xu and M. P. Anantram, *Senior Member, IEEE*

***Abstract*— Resistive switching behavior has been experimentally observed in Hafnia-based unipolar memory devices with negative thermophoresis. The traditional mechanism of RESET where the vacancy moves away from the filament fails to explain the reset behavior in these devices. We propose a model for RESET that involves diffusion of oxygen interstitials to break the vacancy-based filament in a region close to the top electrode as opposed to the center of the filament. Using Monte Carlo simulations, we establish the validity of the mechanism and show that it can model SET and retention.**

***Index Terms*— Kinetic Monte Carlo (KMC), resistive random access memory (RRAM), resistive switching.**

I. Introduction

RESISTIVE random access memory (RRAM) devices are a promising route to replace Flash memory with a simple crossbar structure. Recent work also points to the potential of RRAM in neuromorphic computing [1]–[5]. Various reports show that in Hafina-based RRAM devices, the conducting filament is due to oxygen vacancies. Recent experiments have also shown negative thermophoresis in Hafnia devices [6]–[8]. Here, negative thermophoresis is the process by which oxygen vacancies diffusion from colder to hotter regions. In these devices, the mechanism of heat-induced rupture due to the vacancy movement is not a practical mechanism for RESET (transition from low to high resistance state). This is because vacancies move inward toward the hotter filament regions and aggregate; this process only further strengthens the conductance.

With the scaling of devices to smaller dimensions, an understanding of the switching process at the atomistic level is important. In this brief, we present kinetic Monte Carlo (KMC) simulations to investigate the mechanism for the reset process in Hafnia-based devices with negative thermophoresis.

Our model is based on the KMC method, where both diffusions of oxygen vacancies and oxygen interstitials inside Hafnia are considered. We use a simulation framework that was published by us recently [9]. The differences from our prior work are that the memory cell is sandwiched between two inert electrodes (cannot absorb or react with oxygen), the reset is unipolar, and the generation of vacancies and interstitials occurs in a grain boundary region that has a lower formation energy (Fig. 1). The kinetics of vacancies and interstitials are governed by heat and Poisson's equations [9], [10].

A critical part of modeling is the choice of energy barriers for various processes. Their values and the underlying reasons for choosing them are discussed in detail in the following. *Ab initio* calculations show that the formation energy (E_{form}) of a Frenkel pair is around 5–8 eV [11]. From Arrhenius law $t_G = t_0 \exp(E_{\text{form}}/kT)$, at 300 K with the prefactor of $t_0 = 10^{-15}$ s, the average generation time for one Frenkel pair is about 10^{10} s. However, experiments show that switching can happen within 1 ms [2]. Both grain boundaries [10] and mechanical stress [12] can decrease the formation energy. In this brief, to include these results of formation energy lowering, we introduce a grain boundary region with a formation energy of 1.4 eV (which is in between the 3 and 4C values) [13], whereas the formation energy is 6 eV outside. The diffusion barriers are taken to be stress independent. We take the barrier for vacancy diffusion from the low to high formation energy regions to be 4.6 eV, whereas there is no change for the interstitial.

When a voltage is applied, the macroscopic electric field (F) can activate the diffusion of vacancies and interstitials and affect the formation of Frenkel pairs. Since the generation process dominates the time scale for filament formation (t_{form}), in the presence of an electric field, $t_{\text{form}} \sim t_0 \exp((E_{\text{form}} + E_{\text{barr}} - qFd/2)/kT)$. d is the lattice constant of HfO_2 and $q = 2|e|$. On the other hand, the time scale for retention ($t_{\text{retention}}$) is mainly determined by the diffusion barriers (E_{barr}) in the absence of an electric field; therefore, $t_{\text{retention}} \sim t_0 \exp(E_{\text{barr}}/kT)$. If we assume that the diffusion barrier during forming and retention is similar, then we have $t_{\text{retention}}/t_{\text{form}} \sim \exp(qF/2kT)\exp(-E_{\text{form}}/kT)$. With an applied voltage of 2 V, an oxide thickness of $L = 8$ nm, and $d = 0.5$ nm, the approximate ratio of times for retention and formation, ($t_{\text{retention}}/t_{\text{form}}$), is smaller than 148 at 300 K. The highest value occurs when $E_{\text{form}} = 0$. Since experiments show that $t_{\text{retention}}/t_{\text{form}} > 10^8$, the reduction in diffusion rate due to the macroscopic electric field discussed earlier is insufficient to explain the time scale difference

Manuscript received September 2, 2020; revised September 28, 2020; accepted September 28, 2020. This work was supported by Winbond Inc. The review of this article was arranged by Editor P.-Y. Du. *(Corresponding author: M. P. Anantram.)*

The authors are with the Department of Electrical and Computer Engineering, University of Washington, Seattle, WA 98195 USA (e-mail: anant@uw.edu).

Color versions of one or more of the figures in this article are available online at http://ieeexplore.ieee.org.

Digital Object Identifier 10.1109/TED.2020.3028319

0018-9383 © 2020 IEEE. Personal use is permitted, but republication/redistribution requires IEEE permission.
See https://www.ieee.org/publications/rights/index.html for more information.

Authorized licensed use limited to: University of Washington Libraries. Downloaded on November 19,2020 at 19:00:42 UTC from IEEE Xplore. Restrictions apply.

This article has been accepted for inclusion in a future issue of this journal. Content is final as presented, with the exception of pagination.

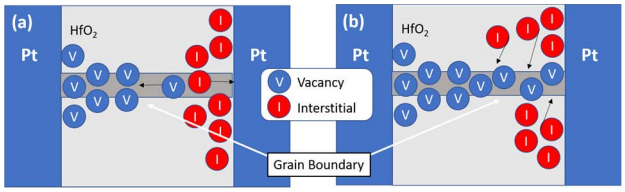


Fig. 1. Illustration of the simulation system. The red and blue circles are oxygen interstitials and oxygen vacancies, respectively. (a) Dark gray region has a lower formation energy for the forming process. The electric field can guide the diffusion of vacancy and interstitial in opposite directions because they are positively and negatively charged, respectively. (b) For the reset process, the interstitial diffusion is primarily toward the hotter filament region due to the concentration gradient.

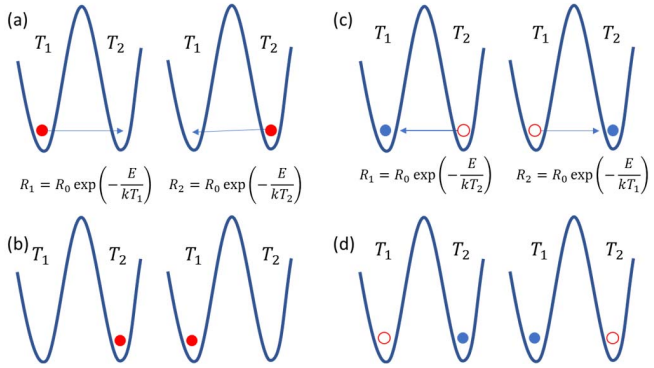


Fig. 2. (a) Initial site of interstitial. (b) Final site of interstitial after diffusion (positive thermophoresis). (c) Initial state of vacancy and lattice oxygen along with the rate for diffusion of lattice oxygen, which is the same as the rate for diffusion of oxygen vacancy. (d) Final site of oxygen vacancy and lattice oxygen after diffusion. The equations imply negative thermophoresis of oxygen vacancies. Red solid circle: interstitial. Red empty circle: lattice oxygen. Blue solid circle: vacancy.

between forming and retention. Two additional factors are as follows:

1) the difference in the diffusion rates during the processes of retention and forming;
2) a much larger Frenkel pair generation rate due to the local electric field in a high k dielectric.

Ab initio calculations estimate the diffusion barrier to be 1.4 eV for a neutral vacancy and 0.9 eV for a neutral interstitial [13]. Duncan *et al.* [14] suggested that the diffusion barrier for a charged vacancy is ~0.8 eV lower than a neutral one. This contributes to a multiplicative factor of $\exp(\Delta E/kT) \sim 2.6\times10^{10}$ in calculating $t_{\text{retention}}/t_{\text{form}}$. To get a more realistic estimate of t_{form}, we note that $E_{\text{form}} = 1.4$ eV corresponds to a Frenkel pair generation time of $\sim 10^9$ s. As per McPherson's theory [15], this time becomes smaller by a multiplicative factor equal to $\exp(-\mathbf{p}\cdot\mathbf{F_{loc}}/kT)$, where $\mathbf{p}$ is the local dipole moment. The local electric field $\mathbf{F_{loc}}$ is related to the macroscopic electric field $\mathbf{F}$ and the relative dielectric constant ϵ_r by $\mathbf{F_{loc}} = (\epsilon_r + 2)\mathbf{F}/3$. For Hafnia, the dielectric constant $\epsilon_r = 25$, and as a result, the local electric field is nine times larger than F. As a result, t_{form} decreases further by a multiplicative factor of $\exp(-9\mathbf{p}\cdot\mathbf{F}/kT)$. Now, utilizing both the increase in the diffusion barrier by $\Delta E \sim 0.8$ eV for a neutral vacancy and reduction in forming time by $\exp(-9\mathbf{p}\cdot\mathbf{F}/kT)$, we find that $t_{\text{retention}}/t_{\text{form}}$ can be larger than 1.31×10^9. This value is more inline with experiments. We note that while this discussion brings out important elements in estimating $t_{\text{retention}}/t_{\text{form}}$, its purpose is to motivate more accurate theoretical and experimental studies to determine various energies barriers and glean an intuitive understanding of the processes.

A major difference from our prior work [10] is also the inclusion of negative thermophoresis for vacancy movement. Before we discuss vacancy diffusion, we state that the rate of interstitial diffusion is

$$R_{\text{Diff}(I)} = R_0 \exp\left[-\frac{E_{\text{barr}(I)} + qFd/2}{kT_i}\right] \tag{1}$$

where R_0 is the attempt frequency and T_i is the temperature of the initial site from which the interstitial hops to a final site after a single hop. The location of the interstitial before and after a single diffusion event is shown in Fig. 2(a) and (b). Here, if the temperature T_1 is higher than T_2, the diffusion rate from the left to right site is higher than the rate from the right to left site, according to (1). As a result, the net diffusion of interstitials will be from hotter to colder regions (left to right). The diffusion of oxygen vacancy in Fig. 2(c) is induced by the diffusion of lattice oxygen, which is located at the destination site of the vacancy [see Fig. 2(d)]. As the diffusion rate of lattice oxygen depends on the temperature of its initial site, the diffusion rate of the vacancy depends on the temperature of the vacancy's final site (which is the initial site of the lattice oxygen). The vacancy diffusion rate depends on the vacancy's final-site temperature (T_f)

$$R_{\text{Diff}(V)} = R_0 \exp\left[-\frac{E_{\text{barr}(V)} - qFd/2}{kT_f}\right]. \tag{2}$$

With (2), vacancies prefer to stay at sites with a higher temperature, in accordance with the negative Soret coefficient, for example, if we have two regions with different temperatures, T_1 and T_2 as shown in Fig. 2(d). If the temperature T_1 is higher than T_2, the vacancy diffusion rate from right to left is higher than the diffusion rate from left to right. As a result, the vacancy is more likely to aggregate in the hotter region. This prevents the dissolution in the reset process, as vacancies stay near the hotter filament region, which contradicts the heat-induced dissolution theory. $E_{\text{barr}(I)}$ and $E_{\text{barr}(V)}$ are the diffusion barriers for interstitials and vacancies, respectively.

In solving the heat equation, the mean free path of the phonon should be considered. Joule heating is induced by the interaction between electrons and phonons, and a length scale of the order of the mean free path is necessary to reach thermal equilibrium. The phonon mean free path in an oxide is estimated from the thermal conductivity (κ) to be $L_{\text{mfp}} = 3\kappa/\text{Cv}$, where C is the heat capacity and υ is the speed of sound. With the parameters of HfO_2, $\kappa = 1.1$ W/(m · K), $C = 1.16$ J/(cm^3 · K), and $\upsilon = 2815$ m/s, we find that the phonon mean free path is approximately 1.12 nm. In reality, the phonon mean free path would be larger than 1.12 nm because optical phonons contribute to heat capacity but not to thermal conductivity [16]. To account for the finite length scale associated with the phonon mean free path, in our calculations, we take the Joule heat dissipated at each grid point (m, n, l) to

Authorized licensed use limited to: University of Washington Libraries. Downloaded on November 19,2020 at 19:00:42 UTC from IEEE Xplore. Restrictions apply.

This article has been accepted for inclusion in a future issue of this journal. Content is final as presented, with the exception of pagination.

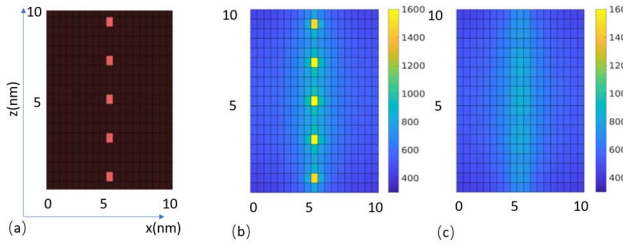


Fig. 3. (a) Steady-state power generated in the red and black regions is 32 μW/nmd and zero, respectively. The red regions mimic resistive regions of the filament here. The steady-state temperature in the filament is obtained by solving the heat equation both (b) without and (c) with considering the phonon mean free path. While the maximum temperature in (b) is over 1600 K, it is below 800 K in (c).

be distributed uniformly on those grid points whose distance to (m, n, l) is less than L_{mfp}. We remark that electrons also relax in the transport direction over a finite length scale, but this is not accounted for explicitly here. As shown in Fig. 3(a), the power density is distributed in several regions (shown in red) inside the oxide layer as several electrons lose their energy at these points in the forming process. Without considering the effect of mean free path, the maximum temperature can be 1600 K or higher, as in Fig. 3(b). On the other hand, with $L_{\text{mfp}} = 1.5$ nm, we find that the maximum temperature in the oxide is reduced to less than 800 K, as shown in Fig. 3(c), that is, the temperature is lower even if the power density is large in a localized region. We take 10% Joule heating in the filament to yield comparable temperatures.

The simulation box is an 8 nm-thick HfO_2 layer with a cross-sectional area of 11 nm $\times$ 11 nm. The central 9 nm^2 region has the formation energy of $E_{\text{form}} = 1.4$ eV, whereas the formation energy is 6 eV outside. An isolated interstitial has a charge of $-2e$ and a diffusion barrier of 0.4 eV. An isolated vacancy has a charge of $+2e$ and a diffusion barrier of 0.6 eV. However, when the vacancy is attached to the bottom electrode or to other neutral vacancies that are electrically connected to the bottom electrode, electrons fill the vacancy energy level and neutralize the vacancy. As said before, such a neutral vacancy has a higher diffusion barrier of 1.4 eV. This is essential for a switching time that is short while making the retention time long. A typical curve of switching current versus time is shown in Fig. 4(a). The applied voltage is 2 V. The current through the memory cell rises at a time of approximately 100 μs when the filament bridges the two electrodes. The current continues to increase until current compliance is reached. Then, the voltage across the device is lowered, which slows down further generation.

In unipolar reset, the polarity of the applied voltage does not change from the set process, but the temperature is larger because there is no current compliance and the applied voltage is smaller. The combination of the change in the charge state of the interstitial due to the applied voltage, which lowers the diffusion barrier and the high temperature due to the absence of current compliance, activates the diffusion process. As a result, the interstitials that have accumulated near the electrode can diffuse actively (Fig. 5). We find that the interstitials diffuse back into the filament due to the concentration gradient and recombine with the vacancies to break the filament

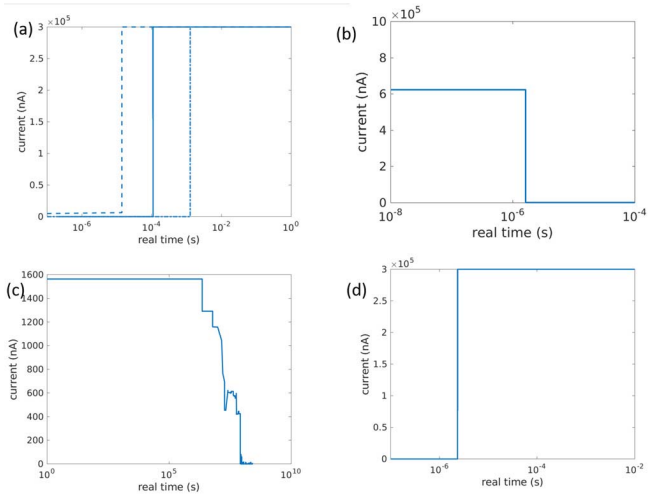


Fig. 4. (a) Current versus time in the processes of form with 8 nm (solid lines). (b) Reset. (c) Retention. (d) Second set process after reset is shown in (b), for an 8-nm-thick oxide (solid lines) at 2-V applied bias. To illustrate the validity of the model, (a) shows the results for oxide thicknesses of 4 nm (dashed) at 2-V applied bias and 12 nm (dotted–dashed) with 2.5-V applied voltage.

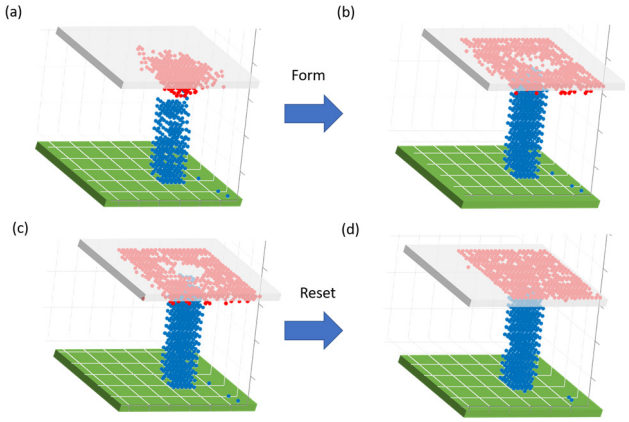


Fig. 5. (a) and (b) Filament shape in the forming process. Interstitials accumulate at the top electrode–oxide interface, and the filament grows and bridges the two electrodes; then, the current increases. (c) and (d) Filament shape in the reset process. The interstitials move as a result of heat and begin recombining with vacancies in the filament; then, the filament breaks at the tip close to the top electrode.

[see black arrows in Fig. 1(b)]. The vacancy–interstitial recombination causes an insulating gap at the top of the filament (Fig. 5), which causes the reset as the resistance increases. We note that the higher temperature also makes the generation rate larger in RESET. A cursory look might seem to say that the generation of new Frenkel pairs would lead to the reformation of the filament, making RESET difficult. However, we find that the smaller local electric field ($\mathbf{F_{loc}}$) due to the smaller applied voltage in RESET makes the vacancy generation process insignificant.

In the absence of an applied voltage, the electric field alone is not enough to create the enormous difference between the retention time and the set time. Since the applied voltage is zero, defects have a large diffusion barrier since they are charge neutral. In our simulations, when the diffusion barrier is 1.2 eV for the neutral interstitial, we find that the device can retain the low-resistance state for more than 10^6 s.

Authorized licensed use limited to: University of Washington Libraries. Downloaded on November 19,2020 at 19:00:42 UTC from IEEE Xplore. Restrictions apply.

This article has been accepted for inclusion in a future issue of this journal. Content is final as presented, with the exception of pagination.

II. Conclusion

We have developed a 3-D model to simulate filament formation, reset, and retention processes in HfO_2-based resistive memory devices with electrodes that do not react with oxygen, under the condition of negative thermophoresis. By detailed numerical simulations, we propose a mechanism for unipolar RESET in a material with a negative Soret coefficient for vacancies. In the unipolar RESET process, the temperature in the filament region is higher than the surrounding region. Under these conditions, negative thermophoresis causes the oxygen vacancies to diffuse into the filament region. In other words, the negative thermophoresis phenomenon eliminates the possibility of filament rupture due to vacancy diffusion alone. Our 3-D simulations show that the filament breaks because of interstitial diffusion close to the electrode as a result of the large concentration gradient. The diffusion of interstitials in the reset process leads to a highly asymmetric breakage of the filament.

Acknowledgment

The authors would like to thank Dr. F. Chen for extensive discussions of the importance of negative thermophoresis devices and the need to capture all three phenomena, set, reset, and retention, using a single model. They also thank J. J. Hsu for useful discussions.

References

[1] R. Waser and M. Aono, "Nanoionics-based resistive switching memories," *Nat. Mater.*, vol. 6, pp. 833–840, Nov. 2007.

[2] F. Pan, S. Gao, C. Chen, C. Song, and F. Zeng, "Recent progress in resistive random access memories: Materials, switching mechanisms and performance," *Mater. Sci. Eng.*, vol. 83, pp. 1–59, Sep. 2014.

[3] T. Hasegawa, K. Terabe, T. Tsuruoka, and M. Aono, "Atomic switch: Atom/ion movement controlled devices for beyond von-Neumann computers," *Adv. Mater.*, vol. 24, pp. 252–267, Jan. 2012.

[4] J. F. Kang *et al.*, "RRAM based synaptic devices for neuromorphic visual systems," in *Proc. IEEE Int. Conf. Digit. Signal Process. (DSP)*, Jul. 2015, Art. no. 12192015.

[5] S. Ambrogio *et al.*, "Neuromorphic learning and recognition with one-transistor-one-resistor synapses and bistable metal oxide RRAM," *IEEE Trans. Electron Devices*, vol. 63, no. 4, pp. 1508–1515, Mar. 2016.

[6] S. Kumar *et al.*, "Conduction channel formation and dissolution due to oxygen thermophoresis/diffusion in hafnium oxide memristors," *ACS Nano*, vol. 10, no. 12, pp. 11205–11210, Dec. 2016.

[7] D. Strukov, F. Alibart, and R. Williams, "Thermophoresis/diffusion as a plausible mechanism for unipolar resistive switching in metal-oxide-metal memristors," *Appl. Phys. A, Solids Surf.*, vol. 107, no. 3, pp. 509–518, 2012.

[8] S. U. Sharath *et al.*, "Control of switching modes and conductance quantization in oxygen engineered HfOx based memristive devices," *Adv. Funct. Mater.*, vol. 27, no. 32, Aug. 2017, Art. no. 1700432.

[9] X. Xu, B. Rajendran, and M. P. Anantram, "Kinetic Monte Carlo simulation of interface-controlled Hafnia-based resistive memory," *IEEE Trans. Electron Devices*, vol. 67, no. 1, pp. 118–124, Jan. 2020.

[10] G. Bersuker *et al.*, "Metal oxide resistive memory switching mechanism based on conductive filament properties," *J. Appl. Phys.*, vol. 110, no. 12, Dec. 2011, Art. no. 124518.

[11] C. Tang and R. Ramprasad, "Point defect chemistry in amorphousHfO_2: Density functional theory calculations," *Phys. Rev. B, Condens. Matter*, vol. 81, no. 16, Apr. 2010, Art. no. 161201.

[12] S. Menzel, P. Kaupmann, and R. Waser, "Understanding filamentary growth in electrochemical metallization memory cells using kinetic Monte Carlo simulations," *Nanosc.*, vol. 7, no. 29, 2015, Art. no. 12673.

[13] S. R. Bradley, A. L. Shluger, and G. Bersuker, "Electron-injection-assisted generation of oxygen vacancies in monoclinic HfO_2," *Phys. Rev. A, Gen. Phys.*, vol. 4, no. 6, Dec. 2015, Art. no. 064008.

[14] D. Duncan, B. Magyari-Kope, and Y. Nishi, "Filament-induced anisotropic oxygen vacancy diffusion and charge trapping effects in Hafnium Oxide RRAM," *IEEE Electron Device Lett.*, vol. 37, no. 4, pp. 400–403, Apr. 2016.

[15] J. W. McPherson, J. Kim, A. Shanware, H. Mogul, and J. Rodriguez, "Trends in the ultimate breakdown strength of high dielectric-constant materials," *IEEE Trans. Electron Devices*, vol. 50, no. 8, pp. 1771–1778, Aug. 2003.

[16] G. Chen, "Thermal conductivity and ballistic-phonon transport in the cross-plane direction of superlattices," *Phys. Rev. B, Condens. Matter*, vol. 57, no. 23, pp. 14958–14973, Jun. 1998.

Authorized licensed use limited to: University of Washington Libraries. Downloaded on November 19,2020 at 19:00:42 UTC from IEEE Xplore. Restrictions apply.